



PAPER

Layered graphene-mica substrates induce melting of DNA origami

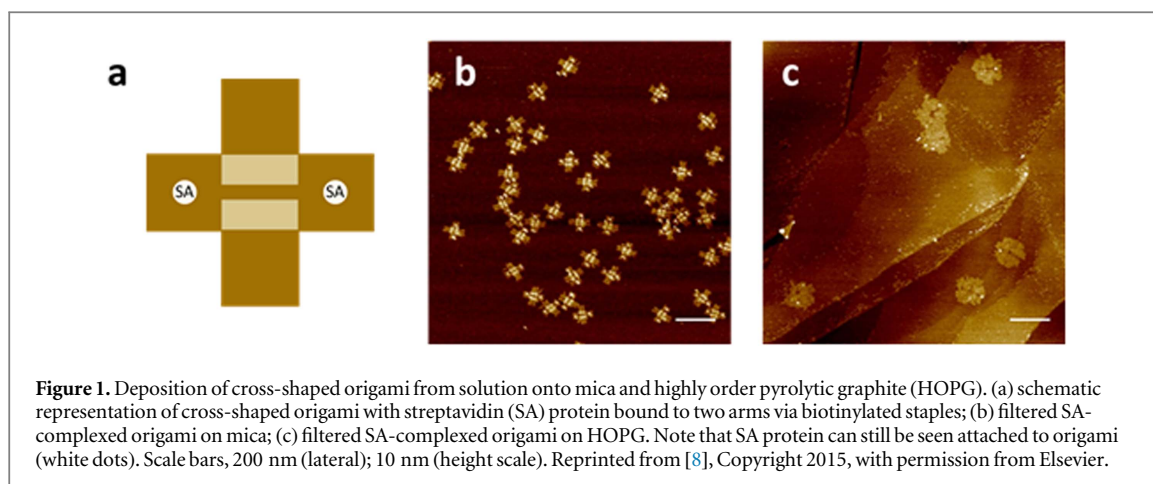
RECEIVED
30 January 2018REVISED
27 March 2018ACCEPTED FOR PUBLICATION
9 April 2018PUBLISHED
20 April 2018Nathaniel S Green¹ , Phi H Q Pham², Daniel T Crow³, Peter J Burke² and Michael L Norton³¹ Department of Natural Sciences, Northeastern State University, Broken Arrow, Oklahoma 74014, United States of America² Department of Electrical Engineering and Computer Science, University of California, Irvine, Irvine, California 92697, United States of America³ Department of Chemistry, Marshall University, Huntington, West Virginia 25755, United States of AmericaE-mail: norton@Marshall.edu**Keywords:** DNA origami, graphene, mica, atomic force microscopySupplementary material for this article is available [online](#)**Abstract**

Monolayer graphene supported on mica substrates induce melting of cross-shaped DNA origami. This behavior can be contrasted with the case of origami on graphene on graphite, where an expansion or partially re-organized structure is observed. On mica, only well-formed structures are observed. Comparison of the morphological differences observed for these probes after adsorption on these substrates provides insights into the sensitivity of DNA based nanostructures to the properties of the graphene monolayer, as modified by its substrate.

Introduction

Graphene has been the focus of intense research particularly after the advent of the chemical vapor deposition (CVD) technique, which allowed for large, device-quality sheets to be formed [1]. These large sheets of graphene have shown great promise in sensing [2–4] and computing applications [5, 6] which derive from graphene's unique physical and electronic properties [7]. Graphene sensors are most commonly constructed by transferring the two-dimensional carbon sheet onto an insulating material, e.g., silicon dioxide, and functionalizing the surface with receptor like structures, e.g., DNA and peptides [8]. Processing reproducibility presents challenges for the production of graphene-based devices in part due to the great care required in order to minimize tearing, folding or wrinkling during transfer [9, 10] and also because the mechanics of biomaterial adsorption on graphene remains poorly understood [4]. A microscopic understanding of the process of biomolecular functionalization of graphene is likely essential to support the production of high-quality sensing devices. Several recent reports have studied the mechanical and electrical properties of exfoliated and CVD graphene transferred onto mica to produce ultra-flat graphene devices [11–14]. Because DNA nanostructures can organize soft molecular species, including molecular receptors, the development of methods to interface them with graphene devices is an extremely appealing objective [15, 16].

DNA origami, nanostructures composed of a long circular ssDNA scaffold shaped by shorter 'staple' strands of ssDNA, have been the focus of intense research interest since 2006 due to their high degree of structural control and nanoscale addressability [17]. To date, these nanostructures have almost exclusively been characterized after deposition on mica substrates. Mica's sub-nanometer surface roughness makes it particularly well-suited for imaging the flexible and often relatively flat/thin DNA assemblies [18]. Moreover, mica has a negative surface charge, which binds well to DNA via dicationic species (Mg^{2+}) in solution through salt bridging [19–21]. Recently, our group and others have been exploring the deposition of DNA origami on different substrates such as gold, silicon nitride, molybdenum disulfide, graphite, and graphene en route to surface functionalized devices [22–27]. Of these materials, graphene is a particularly attractive target for sensor applications but is practically challenging due to the special instability of DNA origami on the carbonaceous sheet [25] which is likely the result of origami's high affinity for graphene due to π - π stacking [28]. Molecular simulation has previously shown that hydrophobic π interactions between nucleotides and graphitic surfaces alter the conformation of DNA [29–32]. In fact, in order to rationalize high density packing of single stranded



DNA on carbon nanotube surfaces, a 2D DNA sheet structure on graphene, a structure which maintains maximal hydrogen bonding and maximizes van der Waals interactions, has been published [33].

Our interest in studying the impact of substrate on these interactions led us to deposit CVD grown graphene on the atomically flat surface of bulk mica in an attempt to take advantage of the hydrophobicity-hydrophilicity ‘transparency’ of graphene, the observation supported both empirically and theoretically, that graphene only partially masks the physical properties of the material it is deposited on [34–36]. It was anticipated that this transparency would reduce the extent of the destabilizing electronic effects of graphite, essentially increasing the localized ‘ionic’ contribution to the binding of the adsorbed origami, thereby preventing the spreading/expansion observed on graphite [27]. Our lab had previously demonstrated that origami pseudo-melts or forms discrete but significantly distorted/expanded forms of its structure when applied to highly oriented pyrolytic graphite (HOPG) (figure 1) [26].

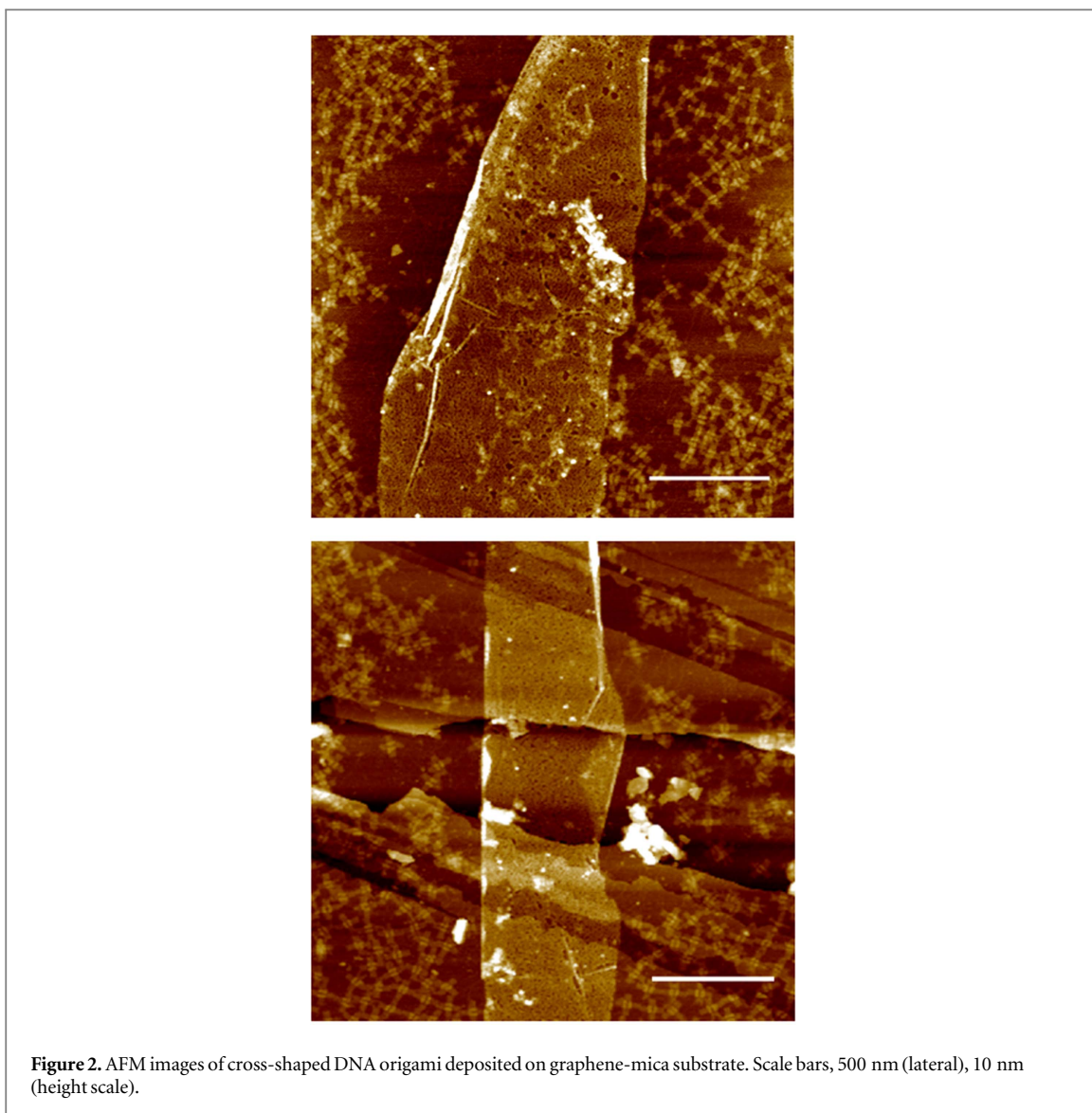
This destabilizing effect was masked if the solution contained excess free DNA or some other species that would passivate the surface [8, 26, 37]. The influence of π -stacking forces on the structure of short ssDNA oligomers adsorbed onto the surface of HOPG leads to a distribution of heights, as visualized using atomic force microscopy (AFM). This observation led the authors to suggest that an energetic crossover in the competition between base-base π stacking and base-graphene π stacking existed, representing a switching point between base stacked DNA and graphene disrupted base pairing [38]. Thus, we expected, due to a diminished graphene π interaction with DNA, that we would observe well-formed structures when filtered DNA origami samples were deposited on graphene perturbed by its mica substrate. Surprisingly, DNA origami was found to be even less stable when adsorbed onto these graphene-mica substrates when compared to adsorption on HOPG.

Here we report the effect of surface-promoted melting of DNA origami adsorbed onto graphene-mica substrates.

Experimental

CVD graphene was transferred onto mica following the standard wet transfer procedure, utilizing a poly(methyl methacrylate) (PMMA) coated graphene layer followed by rinsing in acetone and annealing [39, 40]. Annealing under low pressure and elevated temperature is necessary to remove most of the PMMA from the surface of graphene but presents the possibility of damaging the mica surface with the loss of intercalated water. However, mica was observed by AFM to maintain its flat surface after annealing at 400 °C (figure S1 is available online at stacks.iop.org/MRX/5/045035/mmedia). The resulting sheets of graphene deposited on mica were well-formed with some contamination and structural defects detected by Raman spectroscopy (figure S2). Graphene exhibits two main features in Raman spectra for visible irradiation (532 nm) namely the G ($\sim 1583\text{ cm}^{-1}$) and 2D ($\sim 2685\text{ cm}^{-1}$) bands [41, 42]. Although it has been demonstrated that the position of the G band can be a useful indicator of graphene doping [43–45], interpreting variations in the G band position across the graphene surface due to the interaction of DNA is non-trivial. This is due largely to surface changes, including the possibility of delamination from the substrate, during deposition, and is currently being evaluated as an additional metric for monitoring DNA origami adsorption.

DNA origami solutions were prepared by annealing M13mp18 plasmid with commercially available synthetic oligonucleotide ‘staple’ strands in 1X Tris-acetate-EDTA (TAE) buffer containing 12.5 mM MgCl_2 (origami buffer) slowly from 90 to 20 °C over a 13 h period. The freshly formed origami were then purified with centrifuge membrane columns to remove the excess staple strands that are used to promote high yield origami



formation from the plasmid starting material. The removal of excess staple strands is required, as short ssDNA molecules will readily coat and passivate the graphene surface, preventing observation of the direct interaction of the origami constructs with the bare graphene surface.

Purified origami (8 μl , 1 nM) was adsorbed onto the graphene/mica surface by drop coating with a 1 min incubation at room temperature before a brief rinse with 18 M Ω Millipore water (40 μl) and rapid drying with a stream of nitrogen (figure S3).

Results and discussion

AFM imaging revealed the surface to contain regions of thin strips of graphene and tears within larger graphene sheets, which exposed the underlying mica surface (figures S4–7). These areas provided a unique opportunity to visualize DNA origami on both graphene and mica in the same image. Samples were observed, using AFM, in three conditions: after initial adsorption, after rinsing, and in solution phase. These three conditions were chosen in order to ensure the washing/ drying process was not significantly affecting the apparent degradation of the origami constructs. The same phenomenon, complete disintegration of the origami upon adsorption to graphene, was displayed under all three conditions, over numerous replicates, while the structures that adsorbed onto mica displayed well-formed morphologies.

Figures 2 and 3 show AFM images taken after depositing purified cross-shaped DNA origami onto graphene-mica substrates. Additional AFM images of different sample preparations are available in the supporting information. The AFM images show ‘ribbons’ of graphene, defects formed during deposition and washing of the sample, laying on top of mica with cross-shaped origami deposited on both materials. The

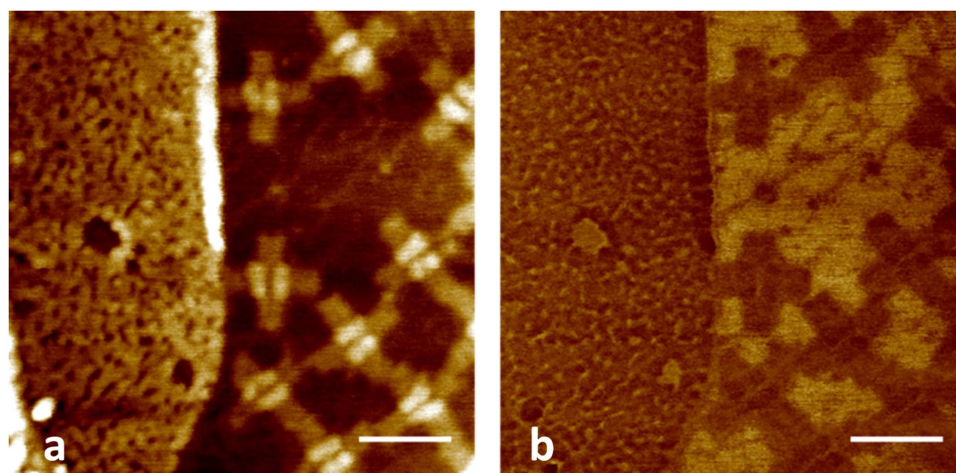


Figure 3. AFM height (a) and phase (b) image of DNA origami deposited on graphene-mica substrate. Scale bars, 100 nm (AFM lateral); 6 nm (height scale); 30 mV (phase).

complete loss of origami structural definition on the graphene-mica regions of the sample is in stark contrast to the expansion and partial deformation observed for origami adsorbed on HOPG (figure 1) [26].

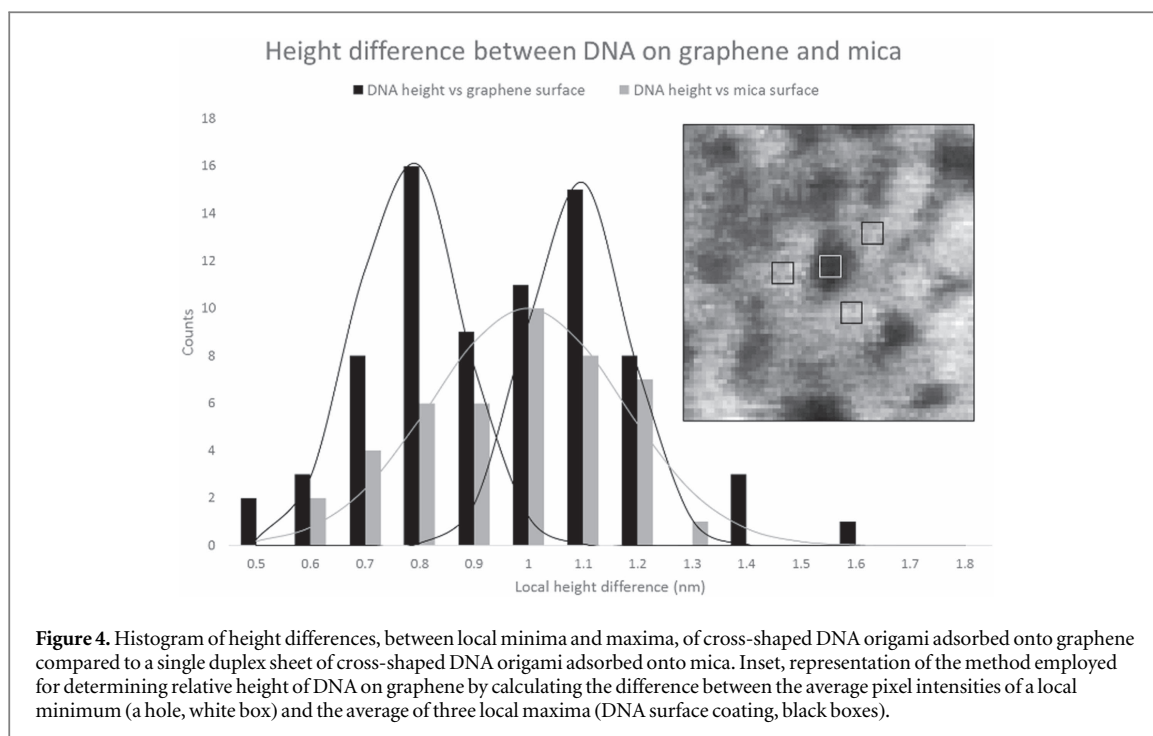
Mica supported graphene dramatically altered the morphology of the adsorbed DNA origami. Only the rough texture of the graphene as compared to the mica surface, visible in the AFM images, serves as evidence of the presence of dis-associated origami based DNA. Furthermore, pristine origami which are visible on the mica revealed by tears in the graphene film are closely juxtaposed with a fibrous network on nearby graphene (figures S5–7). Phase imaging, which yields qualitative surface composition discrimination between different materials, provides further evidence that the material coating the graphene is DNA. The contrast in the phase image (figure 3(b)) is the same for the origami on mica (dark brown) as for the majority of the graphene (left side of figure 3(b)). Similar contrast is apparent in the phase image of figure S5. It may also be noted that material in the holes in the thin DNA film on graphene (figure 3(a)) has mechanical properties similar to mica (dark yellow in figure 3(b)). The complete loss of morphology of the DNA origami is only distinguishable by contrast with the same material on mica.

AFM height analysis has previously been used to probe DNA structure on mica for lattice arrangement, supercoiling, and to distinguish ssDNA from dsDNA [46–48]. Sample preparation and microscope conditions are critical for establishing reproducible and reliable AFM comparisons between experiments [49]. The present approach, scanning over two different surfaces simultaneously under identical temperatures, tip conditions, humidity, etc, overcomes many of these limitations. Here, the height of DNA ‘origami’ can be measured when adsorbed on graphene with respect to the height measured when the intact structures are presented on mica. The relative difference in height, measured by the difference in local minima and maxima of DNA on graphene or mica respectively, is shown in figure 4.

The histogram in figure 4 shows that DNA origami adsorbs under two normally distributed modes on graphene but only one mode for a single layer of cross-shaped DNA origami on mica. Two separate height modes suggest that DNA origami partially melts into ssDNA upon adsorption on graphene. The difference in height average between melted origami on graphene, the lower mode, and duplex DNA on mica (0.2 nm) is in agreement with reported differences for ssDNA versus dsDNA on mica (0.3 nm) [48]. It is important to note that only the single duplex region of the cross-shaped DNA origami, ‘the arms’, were measured on mica in order to probe the relative height of one sheet of duplex DNA. The parallel raised rods at the center of the cross-shape are the result of two DNA duplexes stacked vertically on top of one another (figure S8).

Conclusions

Cross-shaped DNA origami samples are completely melted by interactions occurring during their deposition on the surface of graphene supported by mica. Structures which adsorbed onto the surface of mica maintained their well-defined cross shape while those that adsorbed onto graphene were disassembled. Graphene, and analogously HOPG, have previously been reported to cause deformations of DNA origami [8, 25, 26]. Origami structures are typically imaged on mica due to its atomically flat surface and an apparently stabilizing yet immobilizing ionic interaction with the DNA phosphate backbone. Although it may seem counter intuitive that applying graphene to mica would result in complete destruction of the well-formed origami morphology in view



of the fact that graphene has been reported to be partially ‘transparent’ to the properties of its underlying substrate. These observations suggest that, when on HOPG (multilayer graphene), the strength of the graphene-DNA interaction is reduced by the underlying polarizable, semi-metallic graphite under-layers. This reduced interaction apparently raises the mobility of the ‘staple’ strands dissociated from the origami, and enables distribution of these staples across the surface. While a closely knit network of single stranded DNA expected to result from origami decomposition was not observed in these studies, and may require detailed imaging using scanning tunneling microscopy, models for such hydrogen bonded arrays exist [33] and the observation of hydrogen bonded 2D water structures associated with graphene surfaces provides support for this speculative model [50]. The effect of surface-promoted melting of DNA is important because while carbon based electronic materials are extremely sensitive, they may benefit from high resolution patterning with DNA receptor moieties to impart selectivity and increased multiplexing capabilities for sensing [51]. We hope the results reported here will inspire novel surface passivation and DNA structure stabilization methods that will advance the potential for use of DNA origami as a micro and nanoscale patterning tool on graphene.

Acknowledgments

The authors gratefully acknowledge Dr Masudur Rahman and David Neff for insightful conversations. This research was supported in part by the Army Research Office W911NF-11-1-0024 and W911NF-09-0218 and NSF Cooperative Agreements Numbered EPS-1003907 and OIA-1458952.

ORCID iDs

Nathaniel S Green  <https://orcid.org/0000-0002-1493-0247>

References

- [1] Li X *et al* 2009 *Science* **324** 1312–4
- [2] Wang Y Y and Burke P J 2013 *Appl. Phys. Lett.* **103** 052103
- [3] Mannoor M, Tao H, Clayton J D, Sengupta A, Kaplan D L, Naik R R, Verma N, Omenetto F G and McAlpine M C 2012 *Nat. Commun.* **3** 1761–7
- [4] Lin C T, Loan P T, Chen T Y, Liu K K, Chen C H, Wei K H and Li L J 2013 *Adv. Func. Mater.* **23** 2301–7
- [5] Han S J, Garcia A V, Oida S, Jenkins K A and Haensch W 2014 *Nat. Commun.* **5** 3086
- [6] Schwierz F 2010 *Nat. Nanotech.* **5** 487–96
- [7] Geim A K and Novoselov K S 2007 *Nat. Mater.* **6** 183–91
- [8] Green N S and Norton M L 2015 *Anal. Chim. Acta* **853** 127–42
- [9] Gao L, Ni G X, Liu B, Neto A H and Loh K P 2014 *Nature* **505** 190–4

- [10] Choi J K et al 2014 *ACS Nano* **9** 679–86
- [11] Lui C H, Liu L, Mak K F, Flynn G W and Heinz T F 2009 *Nature* **462** 339–41
- [12] Catellanos-Gomez A, Wojtaszek M, Tombros N, Agrait N, van Wees B J and Rubio-Bollinger G 2011 *Small* **7** 2491–7
- [13] Britton J, Couzens N E A, Coles S W, van Engers C D, Babenko V, Murdock A T, Koos A, Perkin S and Grobert N 2014 *Langmuir* **30** 11485–92
- [14] Low C G, Zhang Q, Hao Y and Ruoff R S 2014 *Small* **10** 4213–8
- [15] Gao Y, Or S, Toop A and Wheeldon I 2017 *Langmuir* **33** 2033–40
- [16] Rahman M, Day B S, Neff D and Norton M L 2017 *Langmuir* **33** 7389–92
- [17] Rothmund P W K 2006 *Nature* **440** 297–302
- [18] Topping T, Voigt N V, Nangreave J, Yan H and Gothelf K V 2011 *Chem. Soc. Rev.* **40** 5636–46
- [19] Bezanilla M, Manne S, Laney D E, Lyubchenko Y L and Hansma H G 1995 *Langmuir* **11** 655–9
- [20] Bustamante C, Vesenka J, Tang C L, Rees W, Guthold M and Keller R 1992 *Biochem.* **31** 22–6
- [21] Pillers M, Goss V and Lieberman M 2014 *Acc. Chem. Res.* **47** 1759–67
- [22] Plesa C, Ananth A N, Linko V, Gulcher C, Katan A J, Dietz H and Dekker C 2014 *ACS Nano* **8** 35–43
- [23] Yun J M, Kim N K, Kim J Y, Shin D O, Lee W J, Lee S H, Lieberman M and Kim S O 2012 *Angew. Chem. Int. Ed.* **51** 912–5
- [24] Scheible M B, Pardatscher G, Kuzyk A and Simmel F C 2014 *Nano Lett.* **14** 1627–33
- [25] Kabiri Y, Ananth A N, van der Torre J, Katan A, Hong J-Y, Malladi S, Kong J, Zandbergen H and Dekker C 2017 *Small* **13** 31
- [26] Rahman M, Neff D, Green N S and Norton M L 2016 *Nanomater.* **6** 11
- [27] Ricardo K B, Xu A, Salim M, Zhou F and Liu H 2017 *Langmuir* **33** 3991–7
- [28] Manohar S, Mantz A R, Bancroft K E, Hui C Y, Jagota A and Vezenov D V 2008 *Nano Lett.* **8** 4365–72
- [29] Zhao X 2011 *J. Phys. Chem. C* **115** 6181–9
- [30] Zhao X, Striolo A and Cummings P T 2005 *Biophys. J.* **89** 3856–62
- [31] Zhao X and Johnson J K 2007 *J. Am. Chem. Soc.* **129** 10438–45
- [32] Zhao X 2008 *J. Phys. Chem. C* **112** 8898–906
- [33] Tu X, Manohar S, Jagota A and Zheng M 2009 *Nature* **460** 250
- [34] Rafiee J, Ji M, Gullapalli H, Thomas A V, Yavari F, Shi Y, Ajayan P M and Koratkar N A 2012 *Nat. Mater.* **11** 217–22
- [35] Raj R, Maroo S C and Wang E N 2013 *Nano Lett.* **13** 1509–15
- [36] Shih C J, Lin S, Park K C, Jin Z, Strano M S and Blankschtein D 2012 *Phys. Rev. Lett.* **109** 049901
- [37] Jin Z, Sun W, Ke Y, Shih C J, Paulus L C, Wang Q H, Mu B, Yin P and Strano M S 2013 *Nat. Commun.* **4** 1663
- [38] Akca S, Foroughi A, Frochtzwajg D and Postma H W C 2011 *PLoS ONE* **6** e18442
- [39] Suk J W, Kitt A, Magnuson C W, Hao Y, Ahmed S, An J, Swan A K, Goldberg B B and Ruoff R S 2011 *ACS Nano* **5** 6916–24
- [40] Ferrari A C et al 2006 *Phys. Rev. Lett.* **97** 187401
- [41] Wang H Q et al 2012 *Nat. Chem.* **4** 724–32
- [42] Dresselhaus M S, Jorio A, Hofmann M, Dresselhaus G and Saito R 2010 *Nano Lett.* **10** 751–8
- [43] Charlier J C, Eklund P C, Zhu J and Ferrari A C 2008 Electron and phonon properties of graphene: their relationship with carbon nanotubes, *Carbon Nanotubes; Topics in Applied Physics* (Berlin: Springer) ISBN 978-3-540-39947-6
- [44] Wang Q, Li Y, Bai B, Mao W, Wang Z and Ren N 2014 *RSC Adv.* **4** 55087–93
- [45] Das A et al 2009 *Nat. Nanotech* **3** 210–5
- [46] Mudalige T K and Sherman W B 2012 *Soft Matter* **8** 3094–104
- [47] Lyubchenko Y L and Shlyakhtenko L S 1997 *Proc. Natl Acad. Sci.* **94** 496–501
- [48] Berg F, Wilken J, Helm C A and Block S 2015 *J. Phys. Chem. B* **119** 25–32
- [49] Lyubchenko Y L 2011 *Micron* **42** 196–206
- [50] Bampoulis P, Teernstra V J, Lohse D, Zandvliet H J W and Poelsema B 2016 *J. Phys. Chem. C* **120** 27079–84
- [51] Lu Y, Goldsmith B R, Kybert N J and Johnson A T C 2010 *Appl. Phys. Lett.* **97** 083107